Bulletin of the Seismological Society of America, Vol. 100, No. 2, pp. 532–540, April 2010, doi: 10.1785/0120090175

Localized Surface Disruptions Observed by InSAR during Strong Earthquakes in Java and Hawai‘i

by Michael Poland

Abstract Interferometric Synthetic Aperture Radar data spanning strong earthquakes on the islands of Java and Hawai‘i in 2006 reveal patches of subsidence and incoherence indicative of localized ground failure. Interferograms spanning the 26 May 2006 Java earthquake suggest an area of about 7.5 km^2 of subsidence (~2 cm) and incoherence south of the city of Yogyakarta that correlates with significant damage to housing, high modeled peak ground accelerations, and poorly consolidated geologic deposits. The subsidence and incoherence is inferred to be a result of intense shaking and/or damage. At least five subsidence patches on the west side of the Island of Hawai‘i, ranging 0.3–2.2 km^2 in area and 3–8 cm in magnitude, occurred as a result of a pair of strong earthquakes on 15 October 2006. Although no felt reports or seismic data are available from the areas in Hawai‘i, the Java example suggests that the subsidence patches indicate areas of amplified earthquake shaking. Surprisingly, all subsidence areas in Hawai‘i were limited to recent, and supposedly stable, lava flows and may reflect geological conditions not detectable at the surface. In addition, two ‘a‘ā lava flows in Hawai‘i were partially incoherent in interferograms spanning the earthquakes, indicating surface disruption as a result of the earthquake shaking. Coearthquake incoherence of rubbly deposits, like ‘a‘ā flows, should be explored as a potential indicator of earthquake intensity and past strong seismic activity.

Introduction

Strong earthquakes result in different styles of surface deformation. Permanent displacements, sometimes several meters in magnitude, characterize zones within a distance approximately equivalent to the rupture length of the fault (e.g., Sieh *et al.*, 1993). An earthquake can also trigger localized mass movement and ground failure at a range of distances from the epicenter. The 2002 Denali earthquake in Alaska, for example, caused rockfalls and rockslides within a few tens of kilometers of the fault rupture and liquefaction several hundred kilometers distant (Harp *et al.*, 2003).

The identification of areas that are prone to localized ground failure and amplified shaking is important to earthquake hazards assessment, but such areas are often not resolvable by seismic and geodetic networks during earthquakes due to insufficient spatial resolution. Radar interferometry (Interferometric Synthetic Aperture Radar [InSAR]) provides spatially contiguous coverage of centimeter-scale deformation along the radar line of sight (LOS) (e.g., Massonnet and Feigl, 1998) and offers the best means of imaging localized ground failures related to earthquakes. InSAR results from earthquakes in Java and Hawai‘i during 2006, using data from the European Space Agency's Environmental Satellite (ENVISAT), reveal several patches of localized subsidence and incoherence, exemplifying the utility of InSAR as a means of recognizing small regions of ground failure due to amplified earthquake shaking.

26 May 2006 Java Earthquake and Associated Deformation

On 26 May 2006 at 22:54 coordinated universal time (UTC), an M_w 6.4 earthquake struck the south coast of Java, Indonesia (Fig. 1; Global Centroid Moment Catalog, see the Data and Resources section), killing about 6000 people, injuring tens of thousands, and leaving hundreds of thousands homeless (Walter *et al.*, 2008). The earthquake was centered south of the city of Yogyakarta at a depth of about 20 km, although there is some disagreement about the hypocenter location and source fault (Nakano *et al.*, 2006; Walter *et al.*, 2008). No surface ruptures formed as a result of the earthquake, complicating efforts to identify the fault that ruptured (Walter *et al.*, 2008).

InSAR results, processed using a 30-m digital elevation model (DEM) acquired by the Shuttle Radar Topography Mission (SRTM; Farr and Kobrick, 2000) for topographic corrections, that span the earthquake indicate broad, permanent displacements of several centimeters southeast of Yogyakarta along the coast of Java (Fig. 1), presumably related to fault

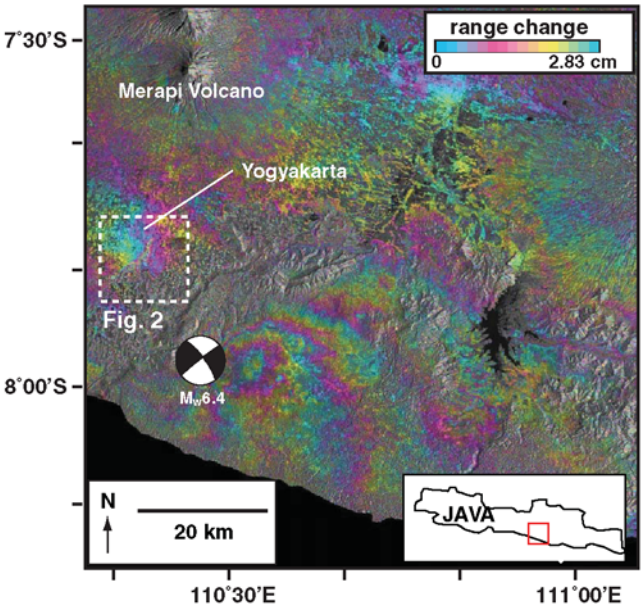

Figure 1. ENVISAT Advanced Synthetic Aperture Radar (ASAR) mode 2, track 318, interferogram spanning 10 May–14 June 2006 and indicating deformation associated with the 26 May 2006 Java earthquake. The earthquake location and focal mechanism are from the Global Centroid Moment Tensor catalog (see the Data and Resources section). The dashed box shows the area of Figure 2.

motion. Immediately south of Yogyakarta is an area of highly localized deformation characterized by subsidence of a few centimeters on its edges, cored by incoherence, and an irregular shape that covers at least 7.5 km^2 (Fig. 2). Interferograms from two independent tracks constrain the deformation to have occurred during 10–29 May 2006. There is no subsidence or incoherence in that region in interferograms that end before or start after 26 May 2006 (Fig. 2), and identical patterns of subsidence and incoherence are present in both tracks, suggesting that the deformation is not a result of atmospheric or data processing artifacts and represents real ground disruption. Further, the localized subsidence and incoherence occurs in a densely populated area and is therefore not related to changes in vegetation. Based on these constraints, the localized subsidence and incoherence south of Yogyakarta are mostly likely a result of the earthquake.

Perhaps not surprisingly, the area of localized surface disruption identified by InSAR coincides with the highest level of damage to housing, greatest modeled peak ground accelerations (3–5 m/sec^2), and reports of especially strong shaking (Nakano *et al.*, 2006; Walter *et al.*, 2007, 2008). The patch of subsidence and incoherence is therefore probably indicative of site amplification of shaking, although the incoherence may also have been caused by building damage, which was considerable in that area (Walter *et al.*, 2008).

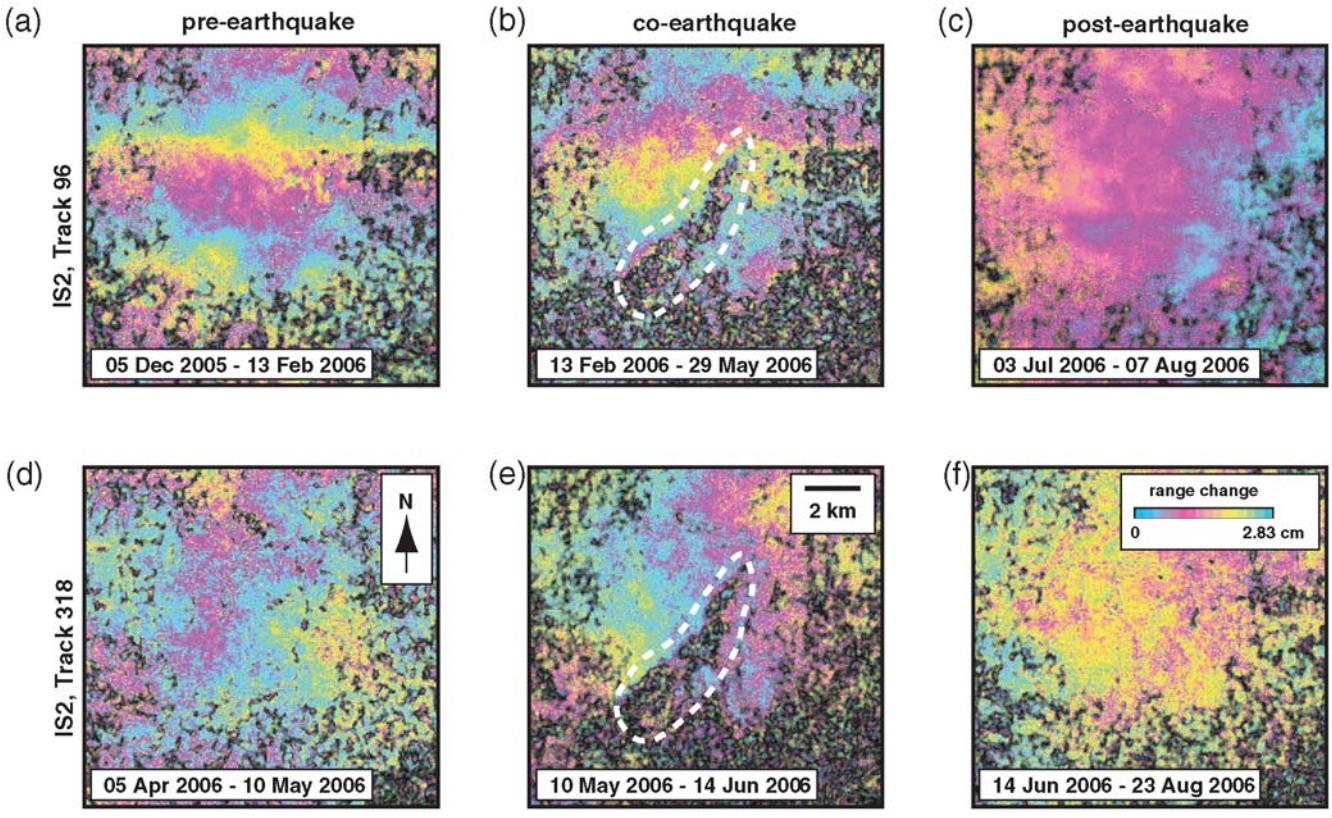

Figure 2. ENVISAT ASAR interferograms spanning time periods (a) and (d) before, (b) and (e) during, and (c) and (f) after the 26 May 2006 earthquake on the south coast of the island of Java. The area covered is shown in Figure 1. Note that the patch of localized subsidence and incoherence (outlined by white dashed lines in parts b and e) is only present in interferograms that span the earthquake. Interferograms have been filtered slightly ($\alpha = 0.1$) using the strategy of Goldstein and Werner (1998) to accentuate the patch of subsidence and incoherence.

15 October 2006 Hawai'i Earthquakes and Associated Deformation

On 15 October 2006, two strong earthquakes occurred at 17:07 and 17:14 UTC on the west side of the Island of Hawai'i (Fig. 3). The first earthquake (designated Kīholo Bay), M_w 6.7, was located beneath Kīholo Bay at a depth of 39 km, and the second earthquake (designated Mahukona), M_w 6.0, was offshore, at 19 km depth, and ~30 km to the north–northeast of the first event (Nakata, 2007; Global Centroid Moment Catalog, see the Data and Resources section). Only minor injuries were reported and structural damage to buildings and infrastructure was light. The lack of severe damage compared to the Java earthquake is probably a result of the greater depths and offshore locations of the Hawai'i earthquakes, different building practices, and lower population density in the epicentral area. No significant regional deformation is apparent in interferograms that span 15 October 2006 (Fig. 3), and no surface rupture occurred. At least five areas of localized subsidence (extending over areas of only 0.3–2.2 km^2), all of which were contained within recent lava flows, were identified on the west side of the island by InSAR results (which, like the Java data, were corrected for topographic effects using the 30-m SRTM DEM).

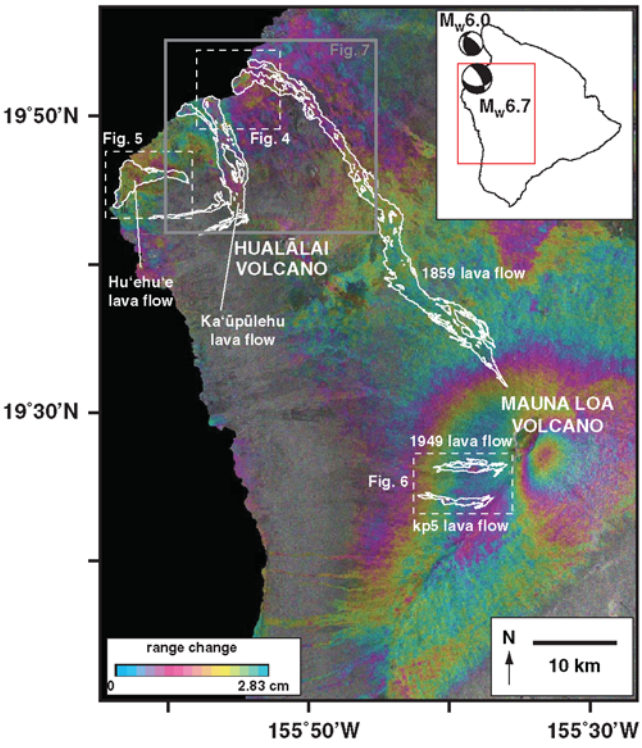

Figure 3. ENVISAT ASAR mode 4, track 157, interferogram spanning 17 February–29 December 2006 and indicating deformation associated with the 15 October 2006 Hawai'i earthquakes. The lava flows discussed in the text are outlined and labeled. The dashed boxes delimit areas covered in Figures 4–6, and the gray box outlines the area of Figure 7. The fringes at the summit of Mauna Loa indicate long-term volcano inflation (confirmed by GPS measurements) and are not related to the 15 October 2006 earthquakes. The inset shows the location of the Kīholo Bay (M_w 6.7) and Mahukona (M_w 6.0) earthquakes, with locations and focal mechanisms from the Global Centroid Moment Tensor catalog (see the Data and Resources section).

The first area (~2.2 km^2 in area and 8 cm LOS maximum magnitude; Fig. 4) was along the northeast margin of Kīholo Bay near the epicenter of the Kīholo Bay earthquake, where the surface is comprised of a lobe of pāhoehoe lava from the 1859 eruption of Mauna Loa Volcano (Rowland and Walker, 1990; Riker *et al.*, 2009) that extended the original coastline (Kauahikaua *et al.*, 1994). Two additional areas of subsidence were a few kilometers to the south (Fig. 5), on the coast immediately west of the Kona International Airport (~2.1 km^2 in area and 6 cm LOS maximum magnitude) and east–northeast of the airport (~0.3 km^2 in area and 3 cm LOS maximum magnitude). Both sites were within the pāhoehoe-dominated Hu'ehu'e lava flow, which erupted from the west flank of Hualālai Volcano in 1801 (Kauahikaua *et al.*, 2002). The coastal subsidence patch was within a portion of the lava flow that created new land (Kauahikaua *et al.*, 1994, 2002).

Subsidence of 3–5 cm LOS occurred at two locations (with areas of ~0.4 and ~1.4 km^2; Fig. 6) within recent 'a'ā flows located high on the southwest flank of Mauna Loa Volcano. One of the flows was emplaced in 1949 (Macdonald and Orr, 1950), while the second, designated kp5 by Lipman and Swenson (1984), is of unknown age but is probably no more than a few hundred years old based on its glassy texture, nominal weathering, and dark color.

In addition to the localized subsidence, portions of both the Ka'ūpūlehu flow, which erupted from the northwest flank of Hualālai Volcano during the eighteenth century (Kauahikaua *et al.*, 2002), and the 1859 Mauna Loa flow (Rowland and Walker, 1990; Riker *et al.*, 2009) are incoherent in interferograms spanning the earthquakes but coherent at all other times (Fig. 7). The change in coherence indicates that the surfaces of the lava flows were disturbed, probably during the earthquakes.

Areas of both localized subsidence and incoherence in west Hawai'i are present in all interferograms that span the 15 October 2006 earthquakes but no interferogams that end before or start after that date (Figs. 4–7), providing strong evidence that the features represent real ground failures and not atmospheric or topographic artifacts. Data spanning the earthquakes are available from 13 independent look angles (3 of which are shown in Figs. 4–6 for illustrative purposes), which constrain the deformation to be dominantly vertical and to have occurred between 2 September and 4 November 2006. Based on their strong spatial and temporal association with the 15 October 2006 earthquakes, the observed ground failures are interpreted to be a result of the seismicity.

No seismic instruments were located within or near the InSAR-recognized ground failures, no felt earthquake reports were made from those regions (which are unpopulated), none of the areas contain roads or other infrastructure that could be

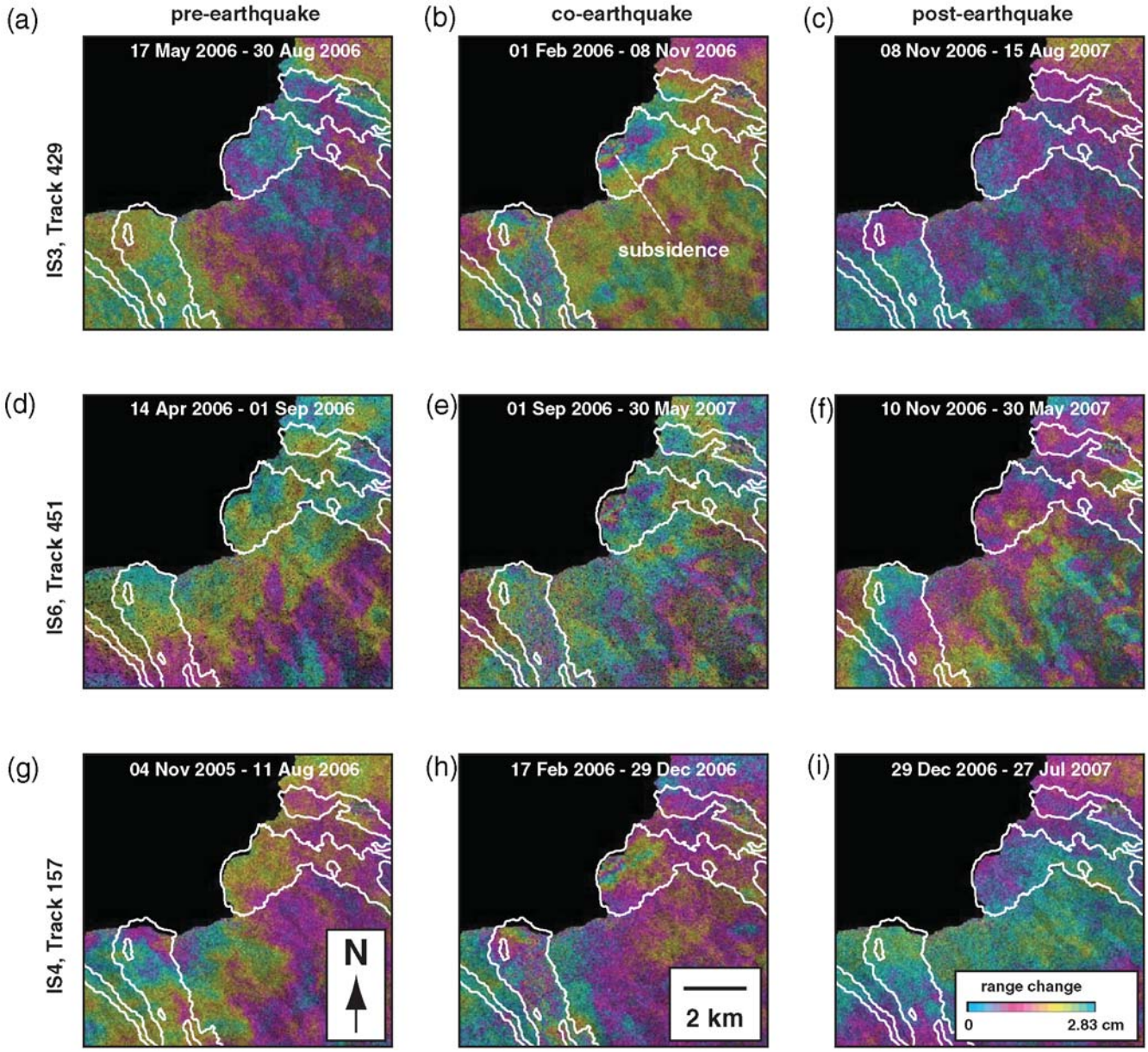

Figure 4. ENVISAT ASAR interferograms spanning time periods (a), (d), and (g) before, (b), (e), and (h) during, and (c), (f), and (i) after the Kīholo Bay and Mahukona earthquakes on 15 October 2006. The area covered is shown in Figure 3. Localized subsidence (indicated in part b) is only present in the interferograms that span the day of the earthquakes. The 1859 Mauna Loa (upper right) and Ka'ūpūlehu (lower left) lava flows are outlined.

inspected for damage, and postearthquake field inspections of all sites showed no obvious manifestations of the localized deformation. As a result, there is no indication of shaking intensities or deformation mechanisms on any of the subsidence areas.

Discussion

Localized Subsidence

Mechanisms to explain the cause of the InSAR-observed localized subsidence must account for two factors: (1) the areas of subsidence were coherent (except for the subsidence core in Java), and (2) the patches occurred in varied environments. The first factor implies that the relative geometry of surface scatterers did not change due to earthquake shaking, but that the ground settled in a coherent fashion by several centimeters. In other words, processes like liquefaction, which would also result in net subsidence, cannot account for the deformation because the surface would not maintain its original characteristics and would be incoherent in radar interferograms. Liquefaction or similar processes may have caused the incoherence in the core of the Java subsidence, although the incoherence might also reflect extreme damage to housing and infrastructure (Walter *et al.*,

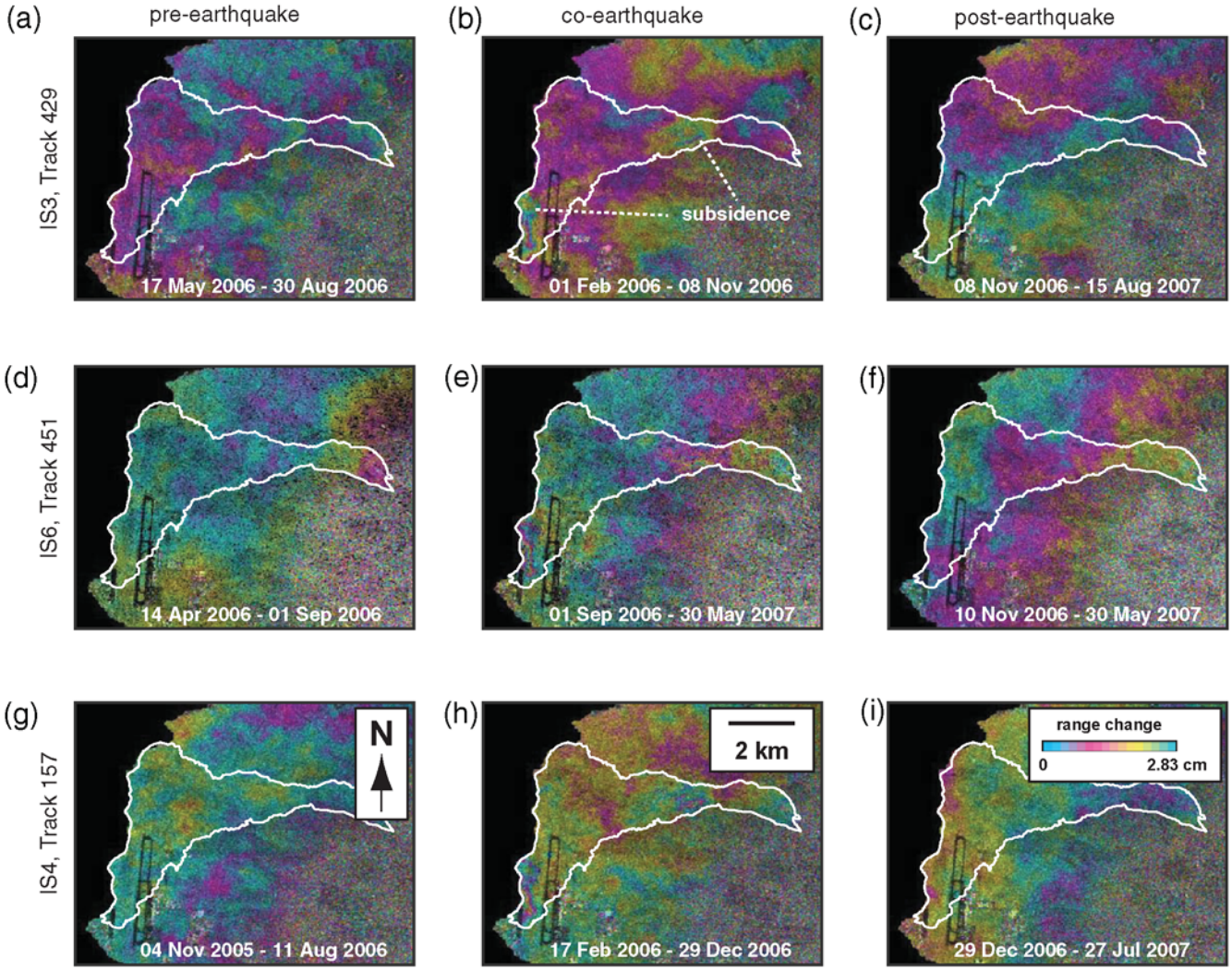

Figure 5. ENVISAT ASAR interferograms spanning time periods (a), (d), and (g) before, (b), (e), and (h) during, and (c), (f), and (i) after the Kīholo Bay and Mahukona earthquakes on 15 October 2006. The area covered is shown in Figure 3. Localized subsidence patches (indicated in part b) are only present in interferograms that span the day of the earthquakes. The Hu‘ehu‘e lava flow is outlined.

2008). The second factor implies that the observed localized ground failures are not a function of distance because there is no correlation between subsidence area or magnitude and distance from the epicenters of either of the Hawai‘i earthquakes.

The cause of subsidence in Java is probably related to near-surface geology. The InSAR-detected disruption south of Yogyakarta occurs in an area of tens to hundreds of meters of loose fluvial and colluvial fill, where earthquake shaking intensities, damage, and modeled peak ground accelerations were relatively high (Nakano *et al.*, 2006; Walter *et al.*, 2007, 2008). Coherence would be preserved along the margins of such an area, with the observed incoherence at the core possibly caused by major surface change and/or heavy damage.

Surprisingly, all localized subsidence patches identified by InSAR in Hawai‘i occurred within recent lava flows, where surface geological conditions would not be expected to amplify shaking. The lava flows, however, may cover shallowly buried, unconsolidated deposits that are more susceptible to earthquake shaking effects. Coastal areas of subsidence in Hawai‘i are on those portions of recent pāhoehoe lava flows that entered the ocean. The new land built by the flows overlies water-saturated debris that was created as lava flowing into the ocean was quenched and shattered (Heliker and Mattox, 2003). Earthquake shaking could induce settling of these shallowly buried littoral deposits, causing the overlying lava flows to sag but maintaining interferometric coherence. Subsidence on the flanks of Hualālai and Mauna Loa cannot be explained by the near-surface occurrence of water-saturated debris but may reflect the presence of near-surface ash, fragmental debris, or other poorly consolidated deposits. Collapse of buried lava tubes during earthquake shaking without associated surface collapse may also explain the noncoastal subsidence patches. About 20–25 cm of localized subsidence, detected by InSAR, was coincident in space and time with the August 2007 collapse

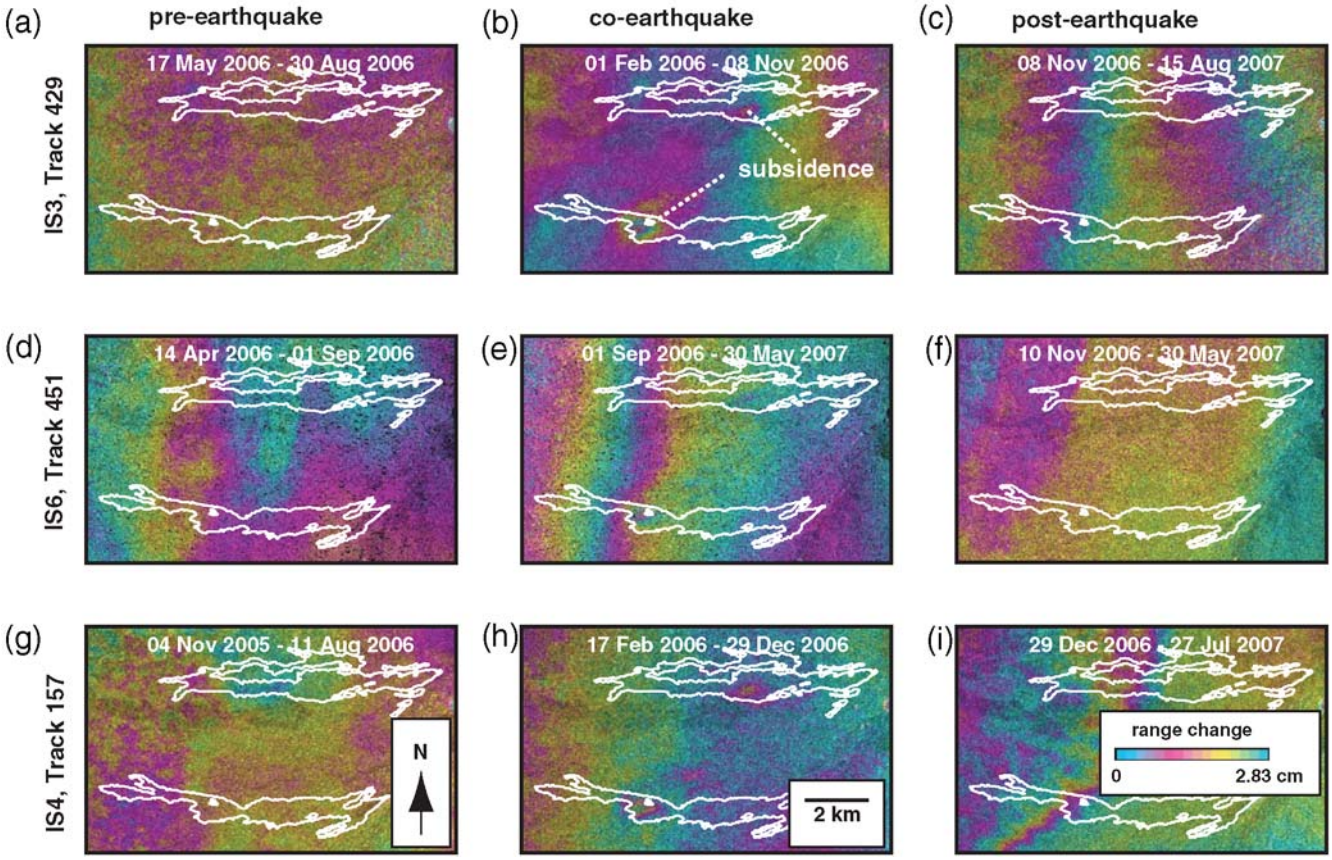

Figure 6. ENVISAT ASAR interferograms spanning time periods (a), (d), and (g) before, (b), (e), and (h) during, and (c), (f), and (i) after the Kīholo Bay and Mahukona earthquakes on 15 October 2006. The area covered is shown in Figure 3. Localized subsidence patches (indicated in part b) are only present in interferograms that span the day of the earthquakes. The 1949 Mauna Loa lava flow (top) and kp5 flow (bottom) of Lipman and Swenson (1984) are outlined.

of an underground mine in Utah (Lu and Wicks, 2008). By analogy, centimeter-scale coherent surface subsidence is a potential consequence of buried lava tube collapse.

While any of these mechanisms could explain the occurrence of subsidence patches within individual lava flow units, no evidence exists to favor one mechanism over another because of a lack of information about subsurface conditions from, for example, drilling or exploration geophysics. Further, field observations from all sites offer no evidence for or against any subsidence cause. The surfaces of all localized subsidence patches show no signs of cracking, collapse, or other phenomena, which is not unexpected given that the patches are coherent (for example, subsurface collapse of a lava tube, which may cause centimeter-scale sagging of the surface, could not have also resulted in surface collapse, because the collapse would have led to incoherence in the interferograms). Observations from subsidence regions high on the flank of Mauna Loa reveal that the 'a'ā flows that host the deformation are characterized by blocks of relatively uniform size (about 25 cm in diameter), but it is unclear if this condition could influence coearthquake subsidence (that is, whether or not earthquake shaking caused these areas to more closely pack, resulting in net subsidence but maintaining coherence). Although the actual mechanism cannot be known given a lack of surface manifestations of the subsidence, all possible mechanisms of localized subsidence in Hawai'i are a consequence of shallow geological conditions, and future work should focus on identifying causal mechanisms based on these constraints.

The recognition of localized subsidence resulting from earthquake shaking has important implications for earthquake hazards and monitoring. Hazards assessments are based in part on surface geology because unconsolidated deposits near the surface amplify earthquake shaking. Localized subsidence in Java was clearly associated with enhanced shaking and, not surprisingly, occurred in an area of poorly consolidated sedimentary deposits (Walter *et al.*, 2007, 2008). Given the apparent similarity of the InSAR-detected subsidence in Hawai'i compared to that in Java, it is probable that the subsidence areas in Hawai'i also indicate areas of amplified shaking, despite the location of all subsidence patches on (supposedly) solid ground (specifically, young lava flows). The 2006 example is not the first time such an apparent contradiction has been noted in Hawai'i. During the 1983 Ka'ōiki earthquake, intense, unexpected shaking was recorded on a recent lava flow in the city of Hilo, which Buchanan-Banks (1987) ascribed to the presence of unconsolidated deposits beneath the stable flow.

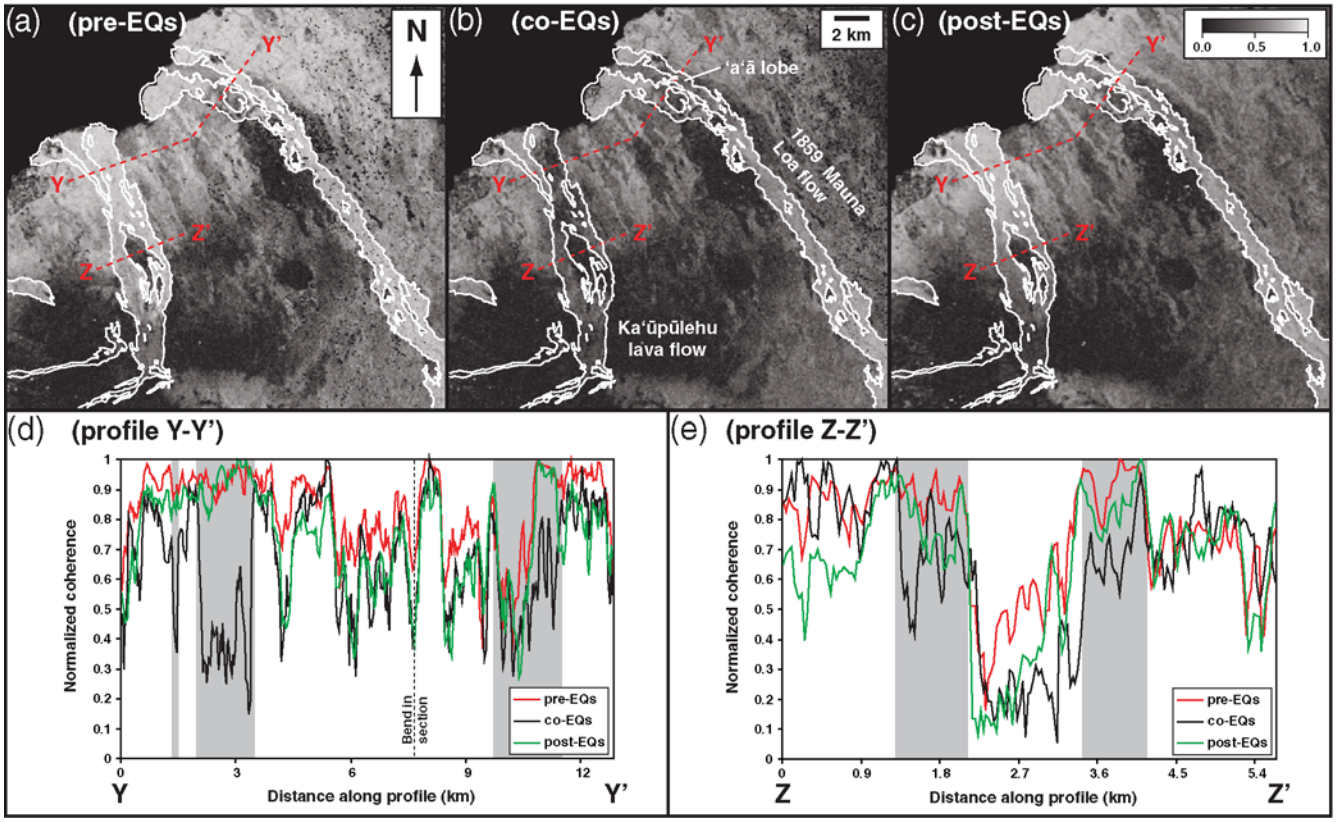

Figure 7. Coherence maps (0.0 = incoherent, 1.0 = coherent) of the Ka'ūpūlehu and 1859 Mauna Loa lava flows (outlined). (a) Preearthquake image spanning 23 June–1 September 2006 from ENVISAT mode 6, track 451. (b) Coearthquake image spanning 1 September–10 November 2006 from ENVISAT mode 6, track 451. (c) Postearthquake image spanning 7 November 2006–27 March 2007 from ENVISAT mode 4, track 408. (d) Normalized coherence along profile Y–Y′ for the three images in parts (a)–(c). (e) Normalized coherence along profile Z–Z′ for the three images in parts (a)–(c). The area covered in parts (a)–(c) is shown in Figure 3. In parts (d) and (e), the gray shaded areas indicate where the profiles pass through the Ka'ūpūlehu and 1859 Mauna Loa lava flows. Coherence in parts (d) and (e) is normalized (that is, actual coherence divided by maximum coherence along the profile) to facilitate comparison between images and highlight differences in relative coherence levels (absolute coherence between images is not comparable due to differences in satellite geometry during image acquisitions). Both the maps and profiles show decreases in coherence across portions of the lava flows in coearthquake imagery relative to preearthquake and postearthquake data. The areas affected include the coastal area of the Ka'ūpūlehu flow (right-hand part of profile Y–Y′), the 'a'ā lobe of the 1859 Mauna Loa flow (left-hand part of profile Y–Y′), and sections of the middle Ka'ūpūlehu flow (profile Z–Z′). Loss of coherence within portions of the lava flows indicates a change in the scattering properties of the surface, probably from reorientation of 'a'ā blocks as a result of earthquake shaking.

Recognition of areas where a thin layer of solid rock is underlain by loose deposits is therefore important to mitigating earthquake hazards.

Identification of regions prone to localized subsidence and amplified shaking during an earthquake is also important for selection of geophysical monitoring sites. Instruments, such as Global Positioning System (GPS) and seismic stations, located in such areas will give results that reflect site effects instead of earthquake source characteristics. Measurements will therefore be inconsistent with other data and may lead to incorrect interpretations of earthquake processes.

Coearthquake Incoherence

Incoherence of the Ka'ūpūlehu and 1859 Mauna Loa lava flows in interferograms spanning the 15 October 2006 earthquakes in Hawai'i (Fig. 7) indicates relative motion of surface scatterers, probably as a result of earthquake shaking. The Ka'ūpūlehu flow is dominated by loose, unfused 'a'ā lava blocks (Kauahikaua *et al.*, 2002), whereas the 1859 Mauna Loa flow is a composite of unfused blocky 'a'ā and smoother pāhoehoe lobes (Rowland and Walker, 1990; Riker *et al.*, 2009). Most of the Ka'ūpūlehu flow and the 'a'ā portion of the 1859 Mauna Loa flow are less coherent in interferograms that span the earthquakes (Fig. 7b) compared to interferograms that end before (Fig. 7a) or start after (Fig. 7c) the earthquakes. The pattern of incoherence on both flows—the only two recent flows with 'a'ā textures in the epicentral area—indicates that the loose, unconnected 'a'ā blocks that characterize the flow surfaces were reoriented during earthquake shaking, thereby changing the scattering properties of the surface. Confirmation that 'a'ā blocks were reoriented based on field observations is, unfortunately, impossible because the flows are unvegetated; thus, it is impossible to tell

whether or not individual 'a'ā blocks have recently moved (the flows in most places are essentially piles of rubble). Nevertheless, the pattern of incoherence on the flows is, by definition, the result of a change in the scattering properties of the surface—a result that is mostly easily achieved by reorienting existing, loose 'a'ā blocks.

Incoherence of disaggregated, rubbly deposits like 'a'ā lava flows may serve as a qualitative indicator of earthquake shaking intensity. Macroseismic data from the Kīholo Bay earthquake indicate Mercalli Intensities of VII–VIII in the area of the Ka'ūpūlehu and 1859 Mauna Loa lava flows (Hopper *et al.*, 2007), suggesting the intensity level exceeded that which was necessary to disrupt the 'a'ā blocks. Extending this observation to the coherence of 'a'ā flows during future earthquakes in Hawai'i (and other seismically active areas with rubbly deposits) may allow for qualitative estimates of shaking intensity and potential use in macroseismic analyses (especially in places where reports of shaking are sparse).

Coherence of rubbly deposits may also provide information about the occurrence of past strong earthquakes. If numerous earthquakes with motions that exceeded the threshold necessary to disrupt the 'a'ā surfaces of the Ka'ūpūlehu and 1859 Mauna Loa lava flows had occurred since the flows were emplaced, the first few such earthquakes might have caused 'a'ā blocks to settle into more stable positions. As a result, coearthquake incoherence would lessen with each succeeding strong earthquake (or it would require stronger and stronger earthquakes to exceed the disruption threshold of the lava flows). The only previous earthquake since 1833 (the start of detailed recording) to reach an intensity of VIII in the area of the Ka'ūpūlehu and 1859 Mauna Loa lava flows was the M 6.5 event of 5 October 1929 (Wyss and Koyanagi, 1992), which, coincidentally, had an intensity distribution similar to the Kīholo Bay earthquake (Hopper *et al.*, 2007). The 1859 Mauna Loa lava flow has therefore experienced only two episodes of VIII-intensity shaking (in 1929 and 2006). The Ka'ūpūlehu flow is of unknown age but probably erupted in the late eighteenth century (Kauahikaua *et al.*, 2002). The paucity of large earthquakes in the northwest part of Hawai'i (Wyss and Koyanagi, 1992) suggests that, like the 1859 Mauna Loa flow, the Ka'ūpūlehu flow also experienced only two ~VIII-intensity earthquakes. If strong earthquakes (with shaking that exceeds the threshold for 'a'ā block reorientation) were more frequent in northwest Hawai'i, surface blocks on the Ka'ūpūlehu and 1859 Mauna Loa lava flows might have already settled into stable positions and the surfaces would have maintained coherence during the 15 October 2006 earthquakes. The number of and strength of earthquakes needed to cause the surface of an 'a'ā lava flow to reach a stable configuration and the role other variables (for example, earthquake source depth and distance, earthquake mechanism, 'a'ā block size, lava flow geometry, etc.) is obviously unknown. Nevertheless, coearthquake coherence variations on the Ka'ūpūlehu and 1859 Mauna Loa lava flows suggest the possibility that coherence measurements on such deposits may be utilized as an indicator of earthquake intensity and past earthquake occurrence and is worthy of additional investigation.

Conclusions

Localized surface disruptions are a significant earthquake hazard and are difficult to detect with point measurements available from GPS, seismic, and other terrestrial monitoring networks. Owing to its excellent spatial resolution, InSAR may be the best tool for recognizing small and isolated areas of ground failure, as demonstrated by the correlation between InSAR-detected subsidence and high levels of damage, modeled peak ground acceleration, and surface geological conditions in Java. By analogy, similar patches of localized subsidence in Hawai'i were probably also associated with amplified shaking, even though all Hawaiian ground failures occurred on recent lava flows that manifested no obvious signs of disturbance based on postearthquake field studies. That apparently stable surfaces, like lava flows, can experience amplified earthquake shaking is probably a reflection of shallow subsurface geological conditions, which may not be apparent from reconnaissance studies and surface geological maps. A test of this hypothesis may be provided by future earthquakes on the seismically active south flank of Kīlauea Volcano in Hawai'i. In 1990, Kaimū Bay was inundated by lava, moving the coastline 300 m seaward (Heliker and Mattox, 2003). The lava flow overlies water-saturated, unconsolidated material that will probably settle during a strong earthquake and cause the stable lava surface to sag, which would be detectable by InSAR.

Coearthquake incoherence of 'a'ā lava flows in Hawai'i indicates that earthquake shaking exceeded the threshold needed to disrupt the lava flow surface. The result suggests that coseisimc interferometric coherence levels on rubbly deposits (like 'a'ā lava flows) are potentially useful as an indicator of earthquake shaking intensities and potentially the history of earthquake shaking in a region—a hypothesis that can be tested at Kīlauea and Mauna Loa volcanoes on the Island of Hawai'i. Both volcanoes host rubbly 'a'ā flows of varying ages and surface characteristics (i.e., different geometries and block sizes) and have experienced numerous strong earthquakes in the past 200 yrs (Wyss and Koyanagi, 1992). During future strong earthquakes, nearby 'a'ā flows may have varying levels of incoherence based on lava flow age, surface characteristics, and location relative to earthquake epicenter, enabling assessment of such observations as a potential tool for inferring the amplitude and duration of earthquake shaking and/or the occurrence of past events.

Data and Resources

InSAR data used in this study were acquired as part of Category-1 Grant 2765 from the European Space Agency, are publicly available, and can be obtained from the European Space Agency or the Western North American

Interferometric Synthetic Aperture Radar (WInSAR) Consortium (for member institutions). Earthquake locations, magnitudes, and focal mechanisms are from the Global Centroid Moment Tensor catalog, searched using www.globalcmt.org/CMTsearch.html (last accessed June 2009). Figures were made using the Generic Mapping Tools software (www.soest.hawaii.edu/gmt; Wessel and Smith, 1998).

Acknowledgments

Jim Kauahikaua and Frank Trusdell provided data and insights related to Mauna Loa and Hualālai Volcanoes. I am grateful for advice, encouragement, and edits from Nick Beeler, Wendy McCausland, and Evelyn Roeloffs. Thanks to Jim Kauahikaua, Jessica Murray-Moraleda, Frank Trusdell, Takeo Jane Takahashi, Patrick McGovern, Francisco Gomez, Matt Pritchard, and an anonymous reviewer for constructive comments.

References

Buchanan-Banks, J. M. (1987). Structural damage and ground failures from the November 16, 1983, Kaoiki earthquake, Island of Hawaii, in *Volcanism in Hawaii*, R. W. Decker, T. L. Wright, and P. H. Stauffer (Editors), *U.S. Geol. Surv. Profess. Pap. 1350*, 1187–1220.

Farr, T. G., and M. Kobrick (2000). Shuttle Radar Topography Mission produces a wealth of data, *Eos Trans. AGU* **81,** 583, 585.

Goldstein, R. M., and C. L. Werner (1998). Radar interferogram filtering for geophysical applications, *Geophys. Res. Lett.* **25,** 4035–4038.

Harp, E. L., R. W. Jibson, R. E. Kayen, D. K. Keefer, B. L. Sherrod, G. A. Carver, B. D. Collins, R. E. S. Moss, and N. Sitar (2003). Landslides and liquefaction triggered by the *M* 7.9 Denali fault earthquake of 3 November 2002, *GSA Today* **13,** 4–10.

Heliker, C., and T. N. Mattox (2003). The first two decades of the Pu‘u ‘*Ō*‘*ō*-Kupaianaha eruption—chronology and selected bibliography, in *The Pu‘u ‘Ō‘ō-Kupaianaha Eruption of Kīlauea Volcano, Hawai‘i—The First 20 Years*, C. Heliker, D. A. Swanson, and T. J. Takahashi (Editors), *U.S. Geol. Surv. Profess. Pap. 1676*, 1–27.

Hopper, M. G., J. W. Dewey, and D. J. Wald (2007). Intensity distribution for the 2006 Kiholo, Hawaii earthquake, *Seism. Res. Lett.* **78,** 297.

Kauahikaua, J., K. V. Cashman, D. A. Clague, D. Champion, and J. T. Hagstrum (2002). Emplacement of the most recent lava flows on Hualālai Volcano, Hawai‘i, *Bull. Volcanol.* **64,** 229–253.

Kauahikaua, J., V. Olmstead, L. Sachnoff, and J. Pallon (1994). Mapping rock walls buried by lava—physical evidence for large, Hawaiian fishponds inundated by 19th century lava flows, *Abstr. Programs Geol. Soc. Am.* **26,** A262.

Lipman, P. W., and A. Swenson (1984). Generalized geologic map of the southwest rift zone of Mauna Loa Volcano, Hawaii, *U.S. Geol. Surv. Misc. Investig. I-1323*.

Lu, Z., and C. Wicks (2008). Study of the 6 August 2007 Crandall Canyon mine (Utah, USA) collapse from ALOS PALSAR InSAR (Abstract G53A-0628), *Eos Trans. AGU* **89,** no. 53 (Fall Meet. Suppl.), G53A-0628.

Macdonald, G. A., and J. B. Orr (1950). The 1949 summit eruption of Mauna Loa, Hawaii, *U.S. Geol. Surv. Bull. 974–A*, 33 pp.

Massonnet, D., and K. L. Feigl (1998). Radar interferomerty and its applications to changes in the Earth’s surface, *Rev. Geophys.* **36,** 441–500.

Nakano, M., H. Kumagai, K. Miyakawa, T. Yamashina, H. Inoue, M. Ishida, S. Aoi, N. Morikawa, and P. Harjadi (2006). Source estimates of the May 2006 Java earthquake, *Eos Trans. AGU* **87,** 493–494.

Nakata, J. (2007). Hawaiian Volcano Observatory seismic data January to December 2006, *U.S. Geol. Surv. Open-File Rept. 2007-1073*, 98 pp.

Riker, J. M., K. V. Cashman, J. P. Kauahikaua, and C. M. Montierth (2009). The length of channelized lava flows: Insight from the 1859 eruption of Mauna Loa Volcano, Hawai‘i, *J. Volcanol. Geotherm. Res.* **183,** 139–156.

Rowland, S. K., and G. P. L. Walker (1990). Pahoehoe and aa in Hawaii—volumetric flow rate controls the lava structure, *Bull. Volcanol.* **52,** 615–628.

Sieh, K., L. Jones, E. Hauksson, K. Hudnut, D. Eberhart-Phillips, T. Heaton, S. Hough, K. Hutton, H. Kanamori, A. Lilje, S. Lindvall, S. F. McGill, J. Mori, C. Rubin, J. A. Spotila, J. Stock, H. K. Thio, J. Treiman, B. Wernicke, and J. Zachariasen (1993). Near-field investigations of the Landers earthquake sequence, April to July 1992, *Science* **260,** 171–176.

Walter, T. R., B. Lühr, M. Sobiesiak, H. Grosser, R. Wang, S. Parolai, H.-U. Wetzel, J. Zschau, C. Milkereit, E. Günther, J. Wassermann, Y. Behr, A. Anggraini, K. S. Brotopuspito, and P. Harjadi (2007). Soft volcanic sediments compound 2006 Java earthquake disaster, *Eos Trans. AGU* **88,** 486.

Walter, T. R., R. R. Wang, B.-G. Luehr, J. Wassermann, Y. Behr, S. Parolai, A. Anggraini, E. Günther, M. Sobiesiak, H. Grosser, H.-U. Wetzel, C. Milkereit, P. J. K. Sri Brotopuspito, P. Harjadi, and J. Zschau (2008). The 26 May 2006 magnitude 6.4 Yogyakarta earthquake south of Mt. Merapi volcano: Did lahar deposits amplify ground shaking and thus lead to the disaster, *Geochem. Geophys. Geosys.* **9,** Q05006, doi 10.1029/2007GC001810.

Wessel, P., and W. H. F. Smith (1998). New, improved version of Generic Mapping Tools released, *Eos Trans. AGU* **79,** 579.

Wyss, M., and R. Y. Koyanagi (1992). Seismic gaps in Hawaii, *Bull. Seismol. Soc. Am.* **82,** 1373–1387.

U.S. Geological Survey—Hawaiian Volcano Observatory
P.O. Box 51
Hawai‘i National Park, Hawai‘i 96718-0051
mpoland@usgs.gov

Manuscript received 10 July 2009